ARCHIVES
of
FOUNDRY ENGINEERING

10.24425/afe.2025.157616

Published quarterly as the organ of the Foundry Commission of the Polish Academy of Sciences

ISSN (2299-2944)
Volume 2025
Issue 4/2025

175 – 189

23/4

Manufacture of Casts Using Replicast CS Technology from Patterns Produced on Injection Molding

K. Łoś [a, b, *], T. Kiczkowiak [b], J. Owczynnikow [b], D. Wojtaszczyk [b], J. Statucki [c], B.P. Pisarek [c], C. Rapiejko [c]

[a] Department of Machine Parts and Mechanism, Faculty of Mechanical Engineering, Technical University of Liberec, Studentská 1402/2, 46117 Liberec, Czech Republic
[b] Polytechnic Faculty, University of Kalisz, Plac Wojciecha Bogusławskiego 2, 62-800 Kalisz, Poland
[c] Lodz University of Technology, Department of Material Engineering's and Production Systems, Poland
* Corresponding author: E-mail: katerina.los@tul.cz

Received 15.10.25; accepted in revised form 19.12.25; available online 31.12.2025

Abstract

The paper discusses issues in the field of casting using the Replicast CS technology and explores the possibilities of applying patterns made on injection moulders with gas injection moulding technology. The scope of the study included designing a Celtic stone pattern and selecting suitable gating system elements based on the analysis of simulation results obtained with MAGMASOFT® v.5.3 software. Determining the dimensions of individual elements, as well as positioning the patterns relative to the pouring gate, was empirical. Changes were made to ensure the production of casts free from defects. Verification focused on parameters such as: solidification temperature, porosity, and metal flow in the mould. After conducting a simulation in MAGMASOFT® v5.3 and achieving satisfactory results, patterns were produced on an injection moulding process, pattern systems were prepared, and ceramic moulds were made. The moulds were then fired, and simultaneously, the patterns were removed from the mould cavities, which were subsequently filled with aluminum alloy AlSi11. An analysis of the quality of the prepared moulds and test casts was also performed.

Keywords: Replicast CS, Simulation of the foundry process, Ceramic moulds, Investment casting, Plastic processing

1. Introduction

The investment casting process is one of the key techniques used to produce precise and complex castings with relatively low mass [1, 2]. Its advantage lies in the fact that a parting surface for the mold is unnecessary, and the internal geometry of the casting can be formed without using cores. This method employs various types of waxes—both synthetic and natural—for creating models. Since waxes typically have melting points above 40°C, the drying temperature of the molds is kept below 23°C. Consequently, the drying time is extended, and in industrial practice, each coating layer usually dries at ambient temperature for about one day. As a result, producing a standard seven-layer mold generally takes around a week.

A process similar to the investment casting method is the Replicast CS technology [3]. In the Replicast CS (ceramic shell) process, wax models are replaced with patterns made from polymer materials that offer high dimensional and shape accuracy and are produced in metal molds. These patterns are assembled into clusters, which are then repeatedly immersed in liquid ceramic mixtures to apply successive layers. After each immersion, the coating undergoes dehydration and drying. When polymer models are used, the drying temperature can be raised to approximately 70°C, which significantly reduces the drying time of each layer. After several coatings, a ceramic shell mold is obtained. The molds are then fired at temperatures between 925°C and 1000°C, during which the polymer pattern burns out, and the ceramic structure becomes hardened.

The Replicast CS method is growing in popularity worldwide as an alternative to the traditional investment casting process, especially for larger castings. As technology develops, requirements for the precision and quality of cast production also increase [4]. Customers demand that the dimensions of their ordered casts closely match the intended design. Nowadays, precision casting is more frequently used in the production of complex elements, which reduces the finishing process time for casts. Research is also being conducted on expanding methods of pattern production. Depending on the chosen production technology, injection moulders, 3D printers, and thermal plotters are increasingly used for this purpose.

The paper presents the possibility of applying patterns made on injection moulders in the gas injection moulding technology Replicast CS.

2. Research methodology

2.1. Materials

For the purpose of study, Celtic stone patterns were designed and then produced using Moplen HP500N [3] with a 2% addition of blowing agent Plastronfoam B20 [4]. The Celtic stone pattern design is presented in Figure 1. Patterns were prepared on the injection moulder ARBURG ALLROUNDER 320 C 500-170 Golden Edition [5].

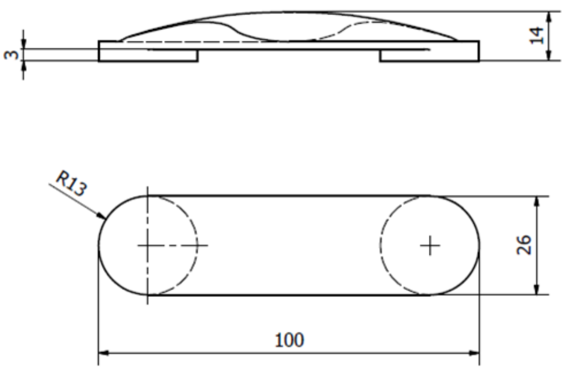

Fig. 1. Celtic stone pattern design

The patterns were produced using a special injection mould with two cavities. The moulding plates are shown in Figure 2. One of them is used to create ellipsoidal shapes, while the other shapes decorative elements, such as inscriptions and logotypes. Additionally, the moulding plates are equipped with a water-cooling system. The external dimensions of the plates are: 240x215x35 mm.

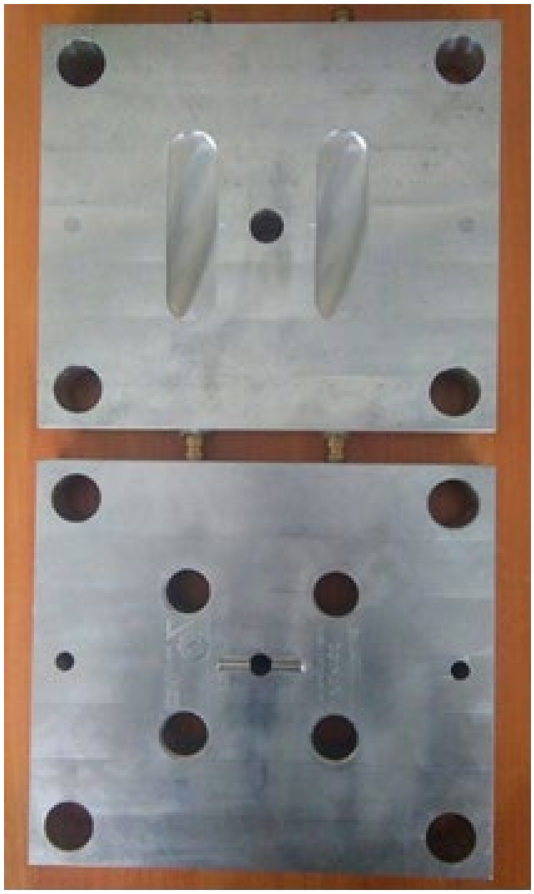
Fig. 2. Plates shaping Celtic stones

Table 1.
Injection parameters for polypropylene with 2% porophor

Injection pressure, bar	Injection time, s	Cooling time, s
1200	0.5	60

The gating system elements (running gates and feeders) were made on 3D printer Zortrax M200 [6] from Z-HIPS [7], material dedicated to the applied printer. The pouring gate was made from frothed polystyrene, with bulk density of 40 kg/m3, on thermal plotter Megaplot P60 [8].

The experimental casts were made in ceramic moulds according to investment casting technology [9]. They consisted of 6 coatings made in mixers and a fluidizer, at the „Armatura" foundry in Łódź, Poland. Appliances used in the process of applying ceramic coatings include mixers and fluidizers [10]. The former are ladles filled with liquid ceramic mixtures, which serve as binder of the ceramic coating. The fluidizers are used to apply the dry element of the mould, i.e. quartz sand of different grain gradations. In the ceramic mould preparation, mixer produced by Perry was used [11]. The described ladle is characterised by 20-litre capacity, rotating around its axis at a rate of 40 rotations/min.

After the pattern system is submerged in binder, it is transferred to the work area of the fluidiser produced by Tridelta [21]. The machine can introduce gas into the lower part of the vessel while simultaneously pouring quartz sand via a pipe located in its upper section. The pneumatic system, with a pressure of 6 atmospheres, is designed to set the dry sand in motion, allowing for more precise application onto the wet pattern system.

Prepared ceramic moulds should be characterised by good gas permeability and adhesive properties. The applied layers consist of a liquid mixture called 'a binder' and a matrix – quartz flour. Table 2 shows the characteristics of coatings of the produced ceramic moulds

Table 2.
Characteristics of ceramic mould coatings

No.	Binder	Flowing power, s	Matrix	Quartz sand granularity, mm
1	Ludox	30	quartz flour	< 0.1
2	Sizol	14 – 15	quartz flour	< 0.1
3	Ethyl silicate	17 – 18	quartz flour	0.4 – 0.8
4	Sizol	18 – 20	quartz flour	0.6 –1.2
5	Ethyl silicate	20 – 24	quartz flour	0.6 – 1.3
6	Ethyl silicate	28 – 30	quartz flour	0.6 – 1.4

The ceramic mould was fired in electric furnace APE 800 [11], which is designed for thermal treatment of ceramic moulds in precision casting. The discussed process was aimed at removing patterns from the inside and giving ceramic coatings appropriate strength.

It can be inferred from the diagram that the mould assigned to cast silumin with the melting point of 577 °C should be fired at minimum of 573 °C. This will ensure the mould's strength and prevent quartz volume growth, thus also preventing cracking during casting. The ceramic mould firing was planned according to the diagram in Figure 3.

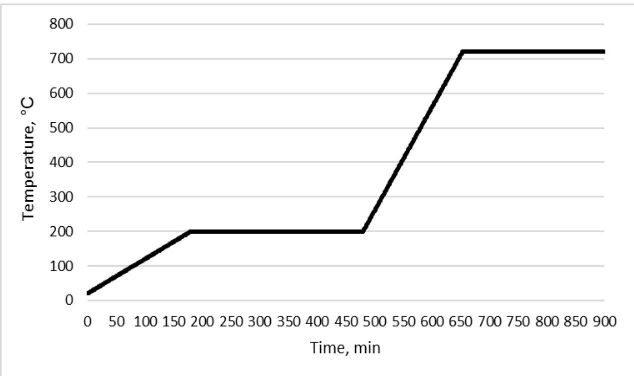

Fig. 3. Diagram of temperature-time dependence during Celtic stone ceramic mould firing

The firing process lasted several hours. Its first cycle ended with stoppage at 200°C, during which patterns were fired inside the mould and the first two β-transformations of quartz occurred in the whole volume. The following temperature increase ended with stoppage at the level of 720°C, during which the quartz sand transformed into α-hexagonal quartz. After that cycle, the mould was removed from the furnace and placed in the casting zone.

Aluminum alloys are often used in foundries, primarily due to their good casting properties, corrosion resistance, excellent mechanical properties at elevated temperatures, abrasion resistance, low coefficient of friction, and thermal expansion [12-17]. The material used to prepare the Celtic stone casts was eutectic silumin AlSi11 [18,19]. The silicon content was 10,9 wt.%. Other elements were also present in the silumin, with the following maximum percentage values: 0,45 wt.% magnesium, 0,05 wt.% copper, 0,4 wt.% manganese, 0,19 wt.% iron, 0,15 wt.% titanium and 0,07 wt.% zinc. The alloy is characterised by good machinability, weldability, hermeticity, corrosion resistance and casting properties [19]. It is applied in elements typical of eutectic silumins, such as valve and carburettor housings, shipbuilding fittings, engine components, tube couplings and various thin-walled casts. The AlSi11 alloy was heated to 850°C in the induction furnace PI30 by Elkon.

The practical part of investigations was preceded by computer simulations of the casting and solidification process in the MAGMASOFT® v5.3. For this purpose, pattern systems were designed.

The selection of the gating system for Replicast CS technology is difficult due to the lack of specified requirements concerning the calculations. Presented below is the preliminary estimation of pouring and running gate for preparation of the Celtic stone [20] in the ceramic mould. Selection of those elements was based on the calculated solidification module, and next on the tables available in the references [4]. The formula for the cast solidification module is presented in equation (1)

$$M = \frac{V}{P} \tag{1}$$

Where: M is solidification module, cm; V is cast volume, cm^3; and P is cast cooling surface area, cm^2.

Equation 1 was used to calculate the cast solidification module M = 0,3 cm. Based on the table available in the references, the diameter and height of the pouring gate (WG) as well as the running gate module (WD) were selected. It can be inferred from the table that the WG diameter should be Φ30 and its height - 300 mm, whereas module WD, for length 8 mm, should equal M = 0,5 cm.

With the assumption that the running gate is cylindrical is shape and with the use of its solidification module, its d = 20 mm was calculated.

2.2. Cast quality evaluation

After the process of casting and metal solidification, the ceramic mould was broken, which made it possible to describe the state of the Celtic stone casts. First of all, such casting defects as contraction cavities, misruns, flashes and deformations needed to be determined. The evaluation also covered the quality of representation of all the surfaces, including the applied decoration elements in the lower part of the cast. Measurements of the overall dimensions of the elements were also performed.

3. Results

This section presents the results of computer simulation studies conducted for four variants of manufacturing cast Celtic stones.

3.1. Variant I

The first variant shows a pattern system with the gating system elements chosen based on initial calculations. The upper gate connects to 6 Celtic stone patterns via cylindrical running gates. The patterns are situated vertically, parallel to the main pouring gate axis. The stones were placed at two heights of the pouring gate and arranged at the angle of 120° in respect of each other, 3 at each level. The pouring gate, Φ30 in diameter, is 320 mm long, whereas the running gates, Φ20 in diameter, have the length of 15 mm. The patterns are connected to the running gates on the side of the flat surface, at the point of their highest thickness. Figures 4, 5 and 6 show the distribution of the patterns and the gating system in different positions.

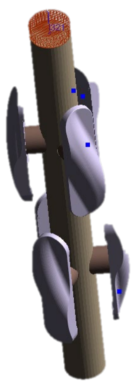

Fig. 4. Variant I Isometric view

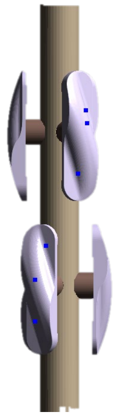

Fig. 5. Variant I Side view

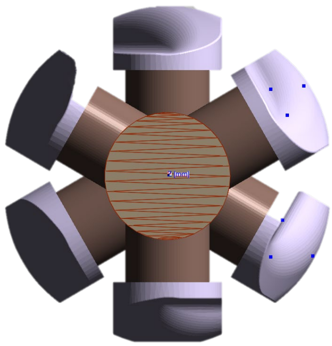

Fig. 6. Variant I Top view

In variant I, the initial conditions were pre-determined by means of the MAGMASOFT® v5.3, the fundamental parameters being as follows:

- Material: AlSi12.
- Pouring time: 6 s.
- Pouring temperature: 650°C.
- Mould preheating temperature: 580°C.

Figure 7 shows the casting temperature after 6 s of casting.

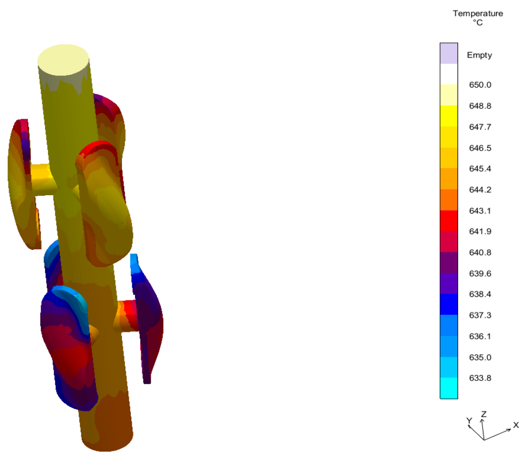

Fig. 7. Celtic stone casting temperature for variant I in 6th second of casting

Figures 8 and 9 shows the metal stream flow in the mould for variant I.

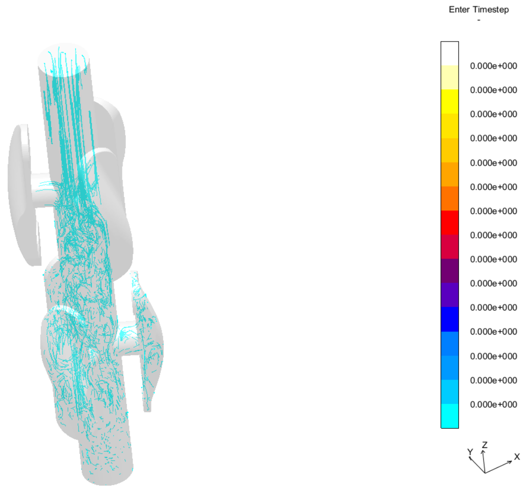

Fig. 8. Celtic stone casting stream for variant one after 3.7 s

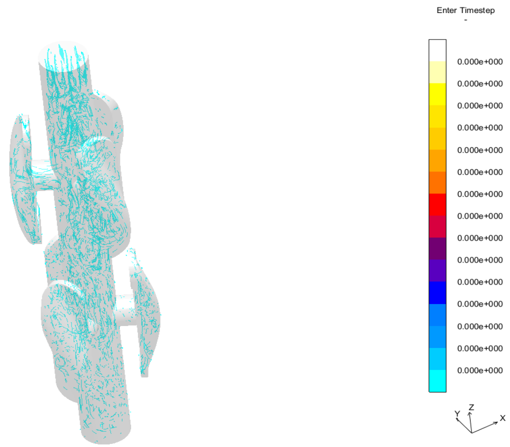

Fig. 9. Celtic stone casting stream for variant one after 6 s

After the performed casting simulation for variant I, temperature changes in the mould as well as a metal stream flow can be observed. It can be inferred from the analysis that the in-flowing liquid, in the first stage, fills the mould cavities of three Celtic stones situated at the lowest levels. That is why these details cool down earlier than the elements located higher levels. Figures 10,11, and 12 show the changes in the liquid fraction during the cast solidification process.

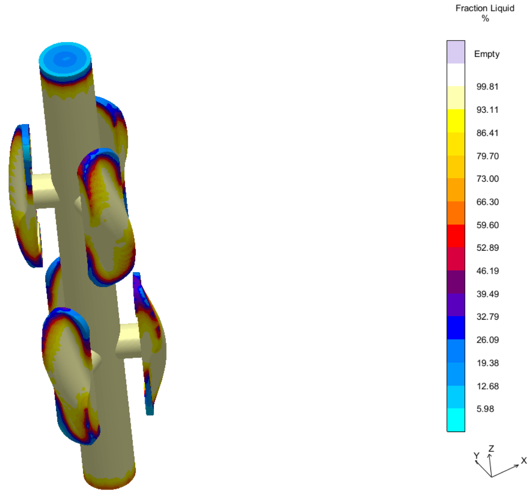

Fig. 10. Liquid fraction during Celtic stone solidification for variant I after 5 min

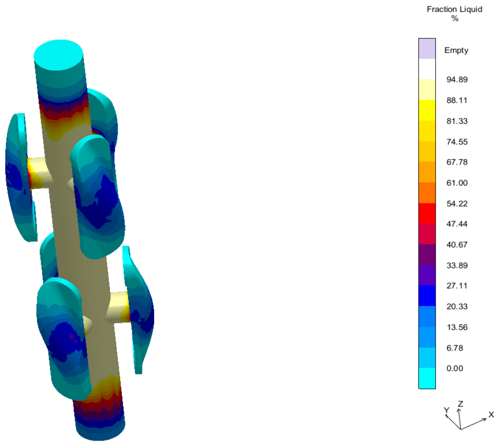

Fig. 11. Liquid fraction during Celtic stone solidification for variant I after 9 min

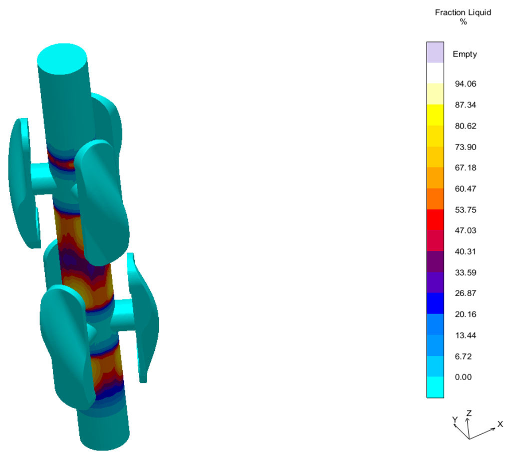

Fig. 12. Liquid fraction during Celtic stone solidification for variant I after 14 min

Figure 13 shows the porosities present in the casts.

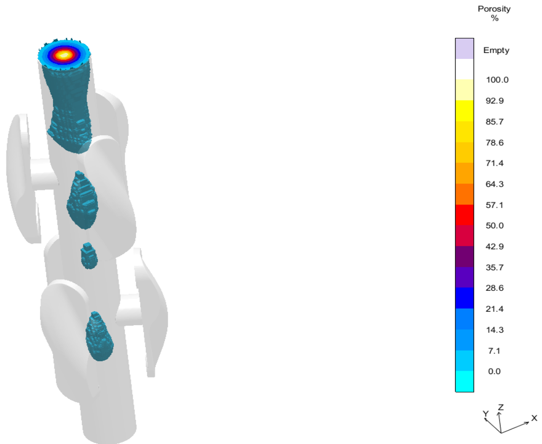

Fig. 13. Porosities on Celtic stone surfaces for variant

During the solidification process analysis, changes of the liquid fraction in the mould and porosities in the casts were observed (Fig. 8). It can be inferred from the analysis that the fastest cooling process takes place in the thin walls of the casts. The liquid fraction, in turn, is maintained for the longest time in the central part of the pouring gate. These are the areas where the formation of porosities is observed. According to the simulation results, they should not occur in Celtic stone casts. Due to the presence of decoration elements in the area of attachment of the running gates, there is no actual possibility to perform casting for this variant. And so, it was necessary to change the place of conveying the gate to the pattern.

3.2. Variant 2

Variant II features a pattern system comprising a pouring gate, nine Celtic stone patterns, and rectangular running gates. The patterns are aligned parallel to the axis of the pouring gate and oriented with their side plane relative to it. The stones are arranged across three levels, with three stones on each level, positioned at 120° angles to one another. The pouring gate, which has a diameter of Φ70 mm, in this variant, measures 300 mm long, whereas the running gates have the following dimensions:

- Width 20 mm,
- Length 30 mm,
- Height 4 mm.

It is possible to calculate the running gate's solidification module from these dimensions, based on equation 1.

$$M = \frac{3 \cdot 2 \cdot 4}{2 \cdot 3 \cdot 0{,}4 + 2 \cdot 3 \cdot 2} = \frac{24}{144} = 0{,}17 \text{ cm}$$

The running gate plane with a lower surface area was connected to the largest flat side surface of the pattern with the height of 11 mm.

Figures 14, 15 and 16 show the distribution of the patterns and the gating system in the analyzed variant.

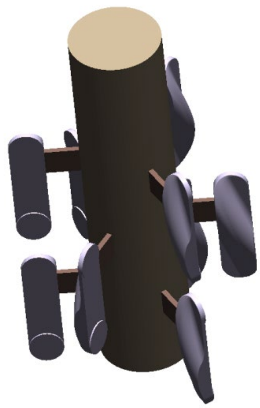
Fig. 14. Variant II Isometric view

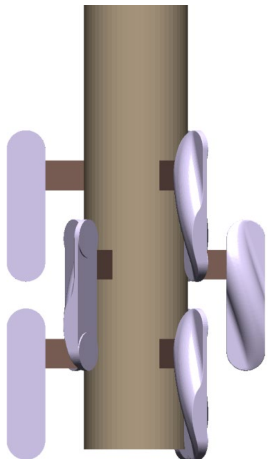
Fig. 15. Variant II Side view.

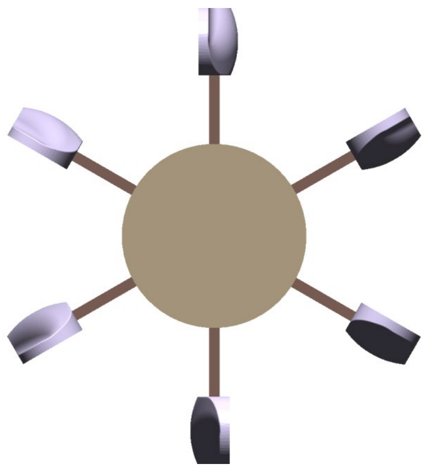
Fig. 16. Variant II Top view

The simulation was performed for modified gating system elements and another location of the patterns. The initial process parameters determined in the MAGMASOFT® v5.3 program remained unchanged. The analysis will include the same properties as in the case of simulation for variant I. Figure 17 shows the metal temperature in the mould after 6 s of casting.

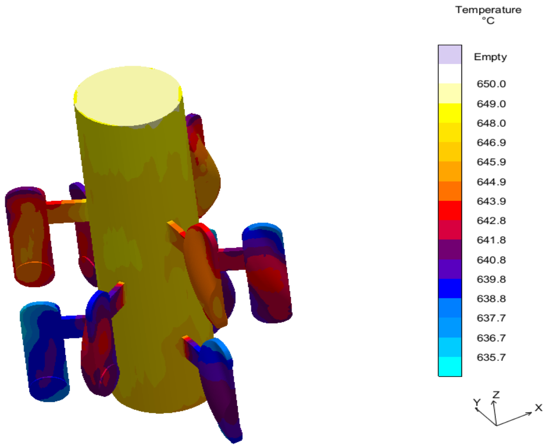

Fig. 17. Celtic stone casting temperature for variant II in 6th second of casting

Figures 18 and 19 show the metal stream (tracers) cast into the mould.

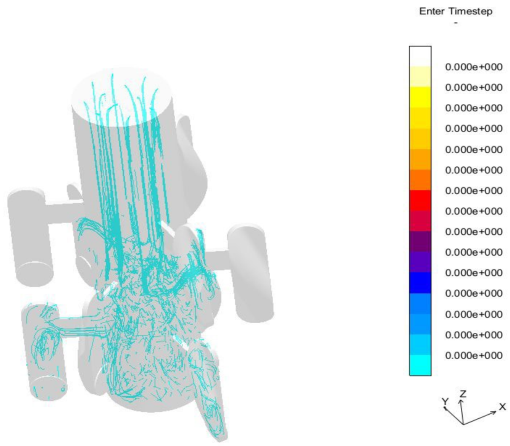

Fig. 18. Celtic stone casting stream for variant II after 3.4 s

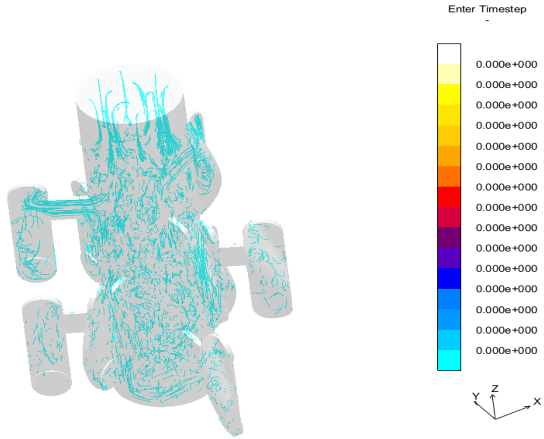

Fig. 19. Celtic stone casting stream for variant II after 5 s

The casting process for variant II runs similarly to the previously analyzed case. In the first place, the cavities located at the lowest level are filled, and they are the ones which initially undergo the solidification process. Figures 20,21 and 22 show the liquid fraction during the metal solidification at different times of the process.

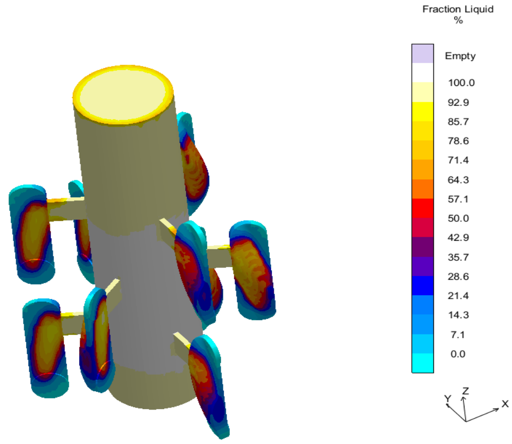

Fig. 20. Liquid fraction during Celtic stone solidification for variant II after 6 min

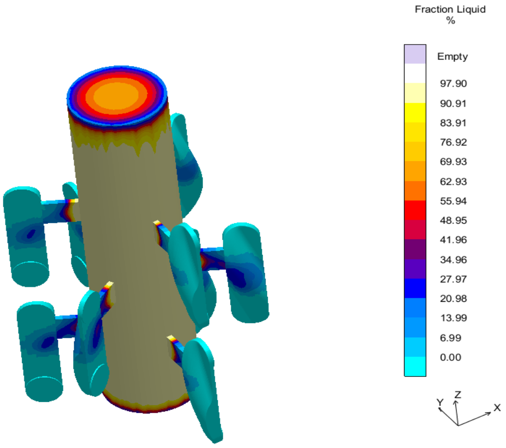

Fig. 21. Liquid fraction during Celtic stone solidification for variant II after 9 min

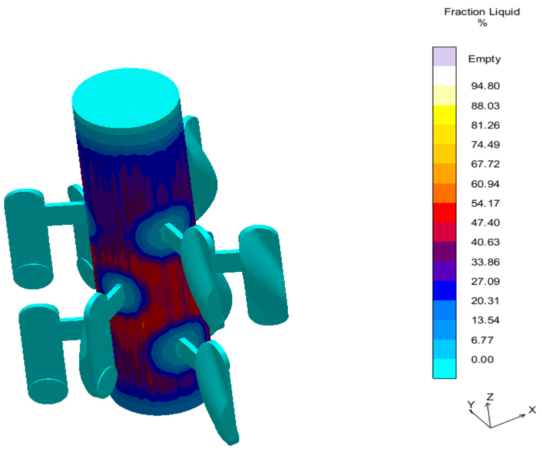

Fig. 22. Liquid fraction during Celtic stone solidification for variant II after 15 min

Figure 23 shows the porosity present in the cast for variant II.

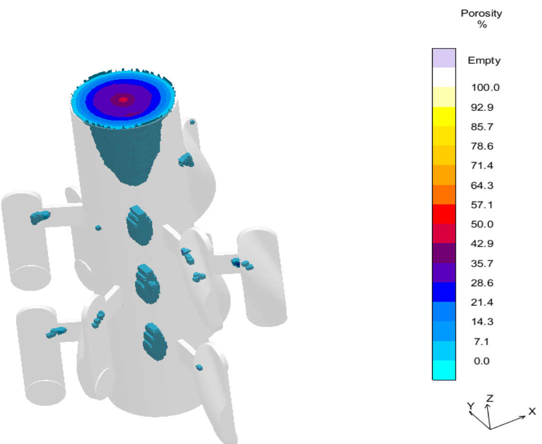

Fig. 23. Porosity on Celtic stone surface for variant II

The analysis of the liquid fraction changes in the casts also confirms the cooling down process of the thin cast walls occurring first. Also, in this case, one can observe the behaviour of the running gates with the solidification module lower than that of the casts. It can be noticed that they begin to solidify earlier – at the moment when thermal units are still present in the casts. This is the reason for the occurrence of porosity in the area where the Celtic stones are joined with the running gates, which has been shown in Figure 21

3.3. Variant III

The third pattern system variant, similarly to the previous case, consists of nine Celtic stone patterns and a similar pouring gate as well as running gates. A difference can be noticed in the manner of arranging the patterns with respect to the pouring gate. In this case, the stones are oriented in the horizontal plane, with their side surface directed towards the pouring gate. Just like in variant II, the running gates are attached to the side flat area. Figures 24, 25, and 26 show the distribution of the pattern system elements III.

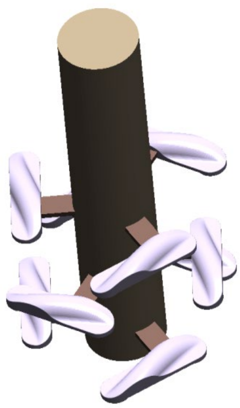

Fig. 24. Variant III Isometric view

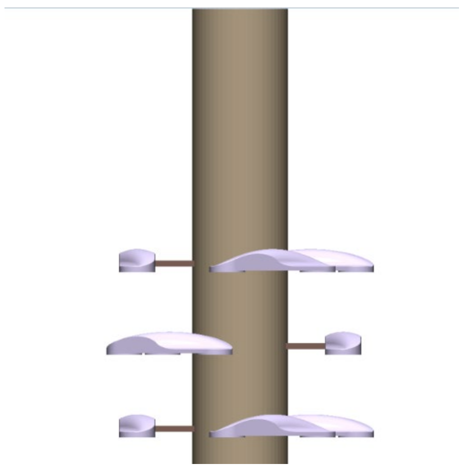

Fig. 25. Variant III Side view

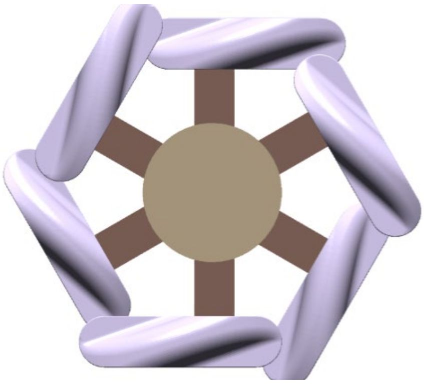

Fig. 26. Variant III Top view

The simulation for variant III was performed with a modified pattern arrangement. In this case, the patterns are situated horizontally, parallel to the XY plane. The casting time was also modified here 5s. The other process parameters remained unchanged. Figure 27 shows the temperature in the 5th second of casting.

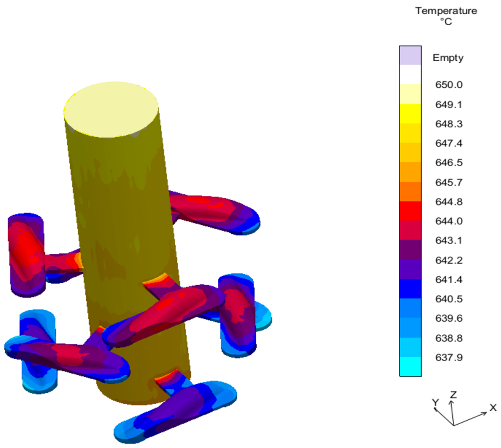

Fig. 27. Celtic stone casting temperature for variant III after 5 s

Figures 28 and 29 show the metal stream flow in the mould.

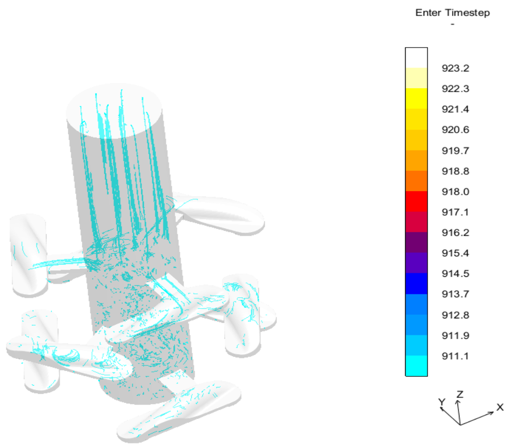

Fig. 28. Celtic stone casting stream for variant III after 3.4s

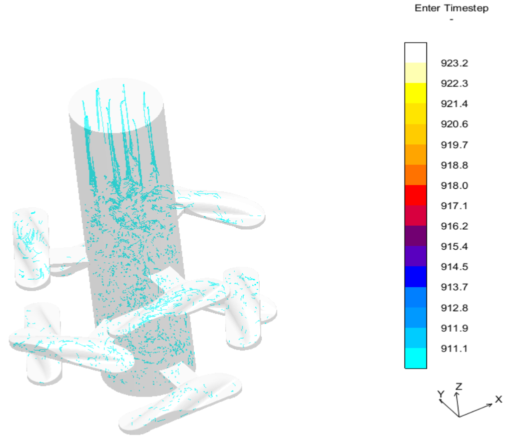

Fig. 29. Celtic stone casting stream for variant III after 5 s

The simulation was performed with slightly modified casting conditions, i.e. with a shortened casting time – down to 5 s. Also, the arrangement of the running gates and the patterns was changed, while the same running gate system element dimensions as in variant II were maintained.

Figures 30, 31, and 32 show the liquid fraction participation during the metal solidification process, whereas in Figure 33, one can see the porosities present in the casts.

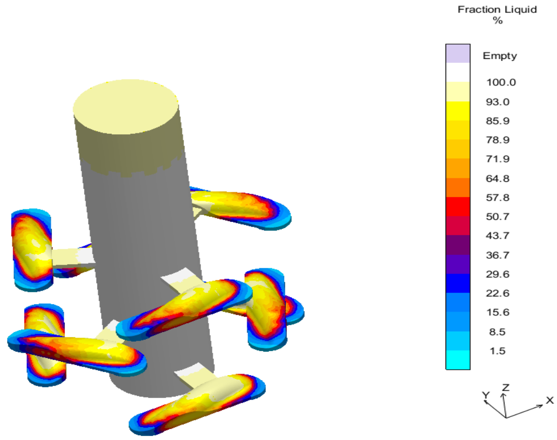

Fig. 30. Liquid fraction during Celtic stone solidification for variant III after 5 min

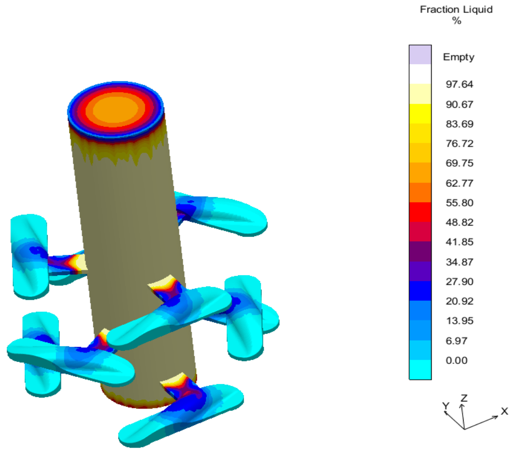

Fig. 31. Liquid fraction during Celtic stone solidification for variant III after 9 min

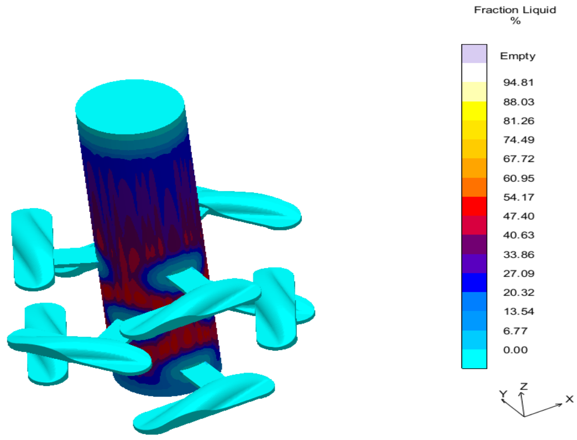

Fig. 32. Liquid fraction during Celtic stone solidification for variant III after 15 s

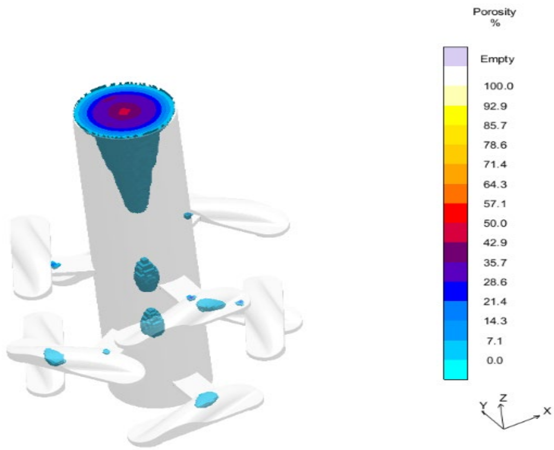

Fig. 33. Porosity on Celtic stone surface for variant III

The analysis of the results shows that the shortened casting time and the distribution of patterns, with the maintained gating system dimensions, do not lead to the elimination of porosity. Also, in this case, one can observe that the metal solidifies in the running gates earlier than in the cast. This is the reason why elements - feeders called 'feed bobs' were used in the following simulation.

3.4. Variant IV

Variant IV is an expanded version of variant III. In this case, to extend the running gate solidification module, additional feed bobs were applied, the dimensions of which are as follows:

- Diameter Φ20
- Height 20mm

The feed bobs were connected to the upper plane of the running gates. The feed bobs used in the presented variant were aimed at delaying the running gate solidification process, thus eliminating the presence of contraction cavities in the casts. Figures 34,35 and 36 show a view of the pattern system IV with the feed bobs

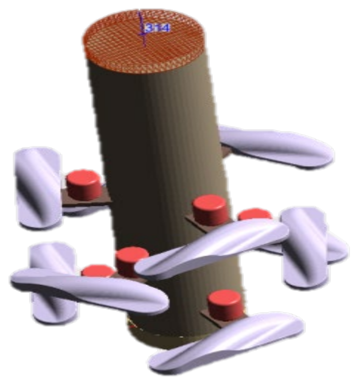

Fig. 34. Variant IV Isometric view

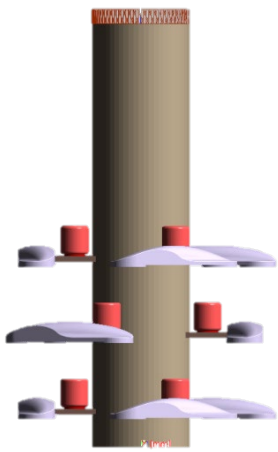

Fig. 35. Variant IV Side view

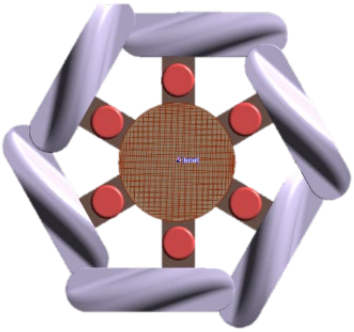

Fig. 36. Variant IV Top view

The simulation was performed on a modified version of variant III. After the analysis of the solidification process, in this case, it was decided to connect the feed bobs to the pouring gate, which aimed at prolonging their solidification time. In consequence, the purpose of this was to eliminate the porosities present in the casts. The simulation took place with modified initial process parameters. Figure 37 shows the casting temperature after 5 s.

Figure 37 shows the casting temperature after 5 s.

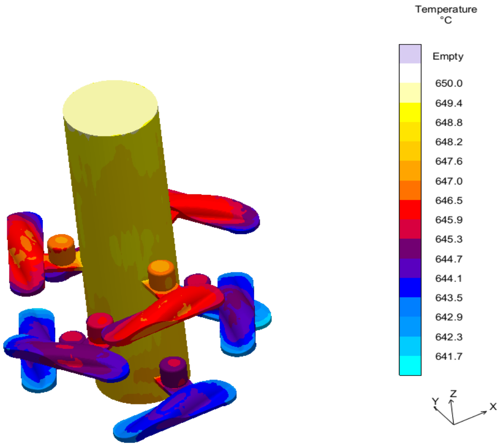

Fig. 37. Celtic stone casting temperature after 5 s for variant IV

Figure 38 shows a schematic metal flow in the mould.

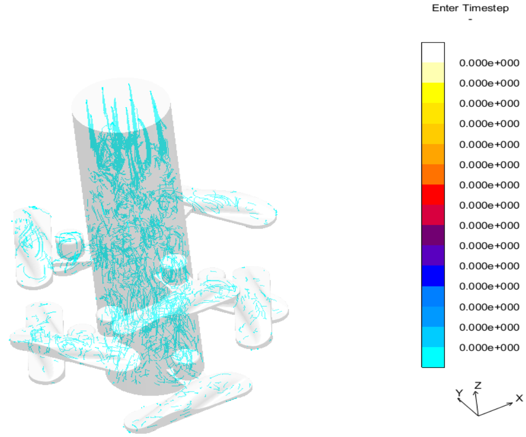

Fig. 38. Celtic stone casting stream for variant IV after 5 s

The figures above illustrate the temperature distribution during the casting process. It is evident that the temperature of the lower casts is lower, which causes the lower part of the mould to fill earlier. Subsequently, the metal flow streams within the mould are shown, confirming the discussed temperature distribution. Figures 39,40 and 41 show the solidification process for variant IV.

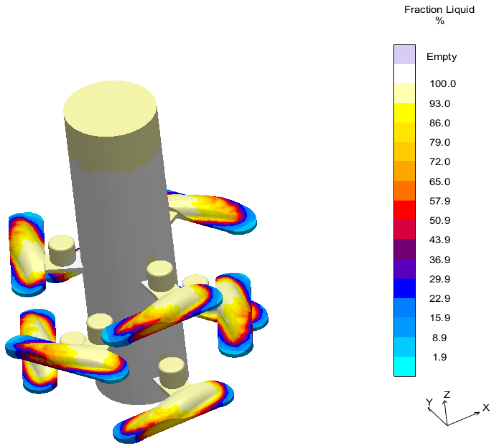

Fig. 39. Liquid fraction during celtic stone solidification for variant IV after 5 min

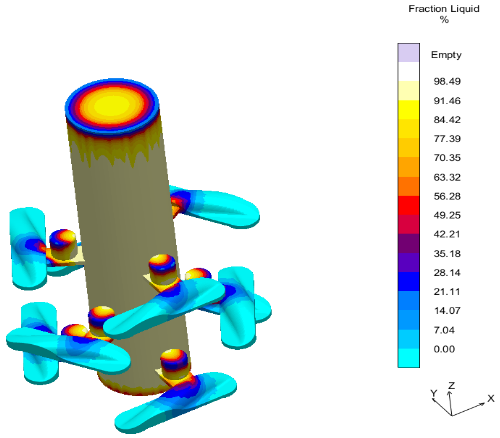

Fig. 40. Liquid fraction during celtic stone solidification for variant IV after 9 min

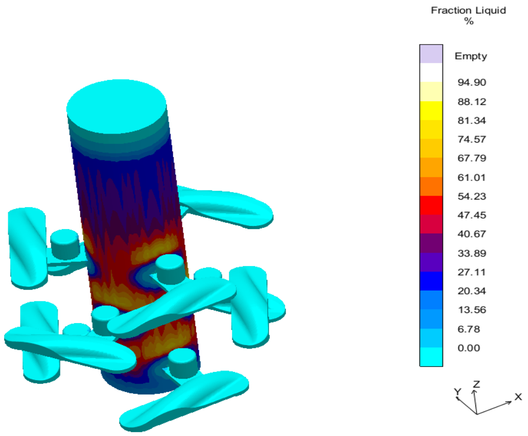

Fig. 41. Liquid fraction during celtic stone solidification for variant IV after 15 min

Figure 42 illustrates the porosities formed in the casts for variant IV.

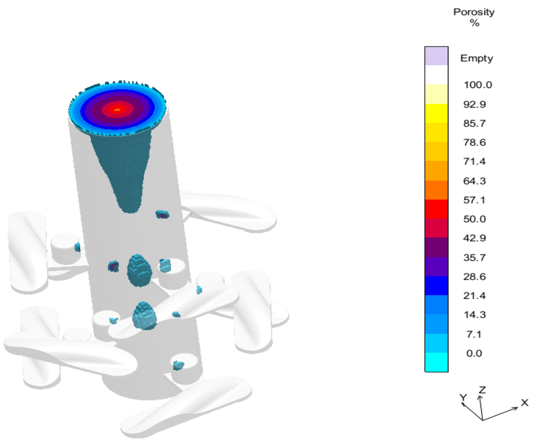

Fig. 42. Porosity on Celtic stone surface for variant IV

The analysis of the liquid fraction change during solidification reveals a difference compared to the earlier described simulation. It is evident that the feeders effectively maintain the running gate temperature during cooling. Consequently, the solidification occurs first in the Celtic stones, followed by the feed bobs and other gating system elements. Figure 42 shows the absence of porosities in the casts, which was a primary assumption of the simulation tests and the selection of the gating system elements.

Figures 43 and 44 show the stresses formed in the casts during the solidification process.

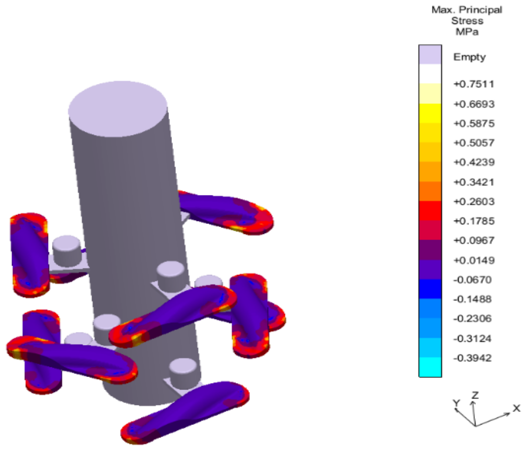

Fig. 43. Stress occurring during solidification for variant IV after 7 min

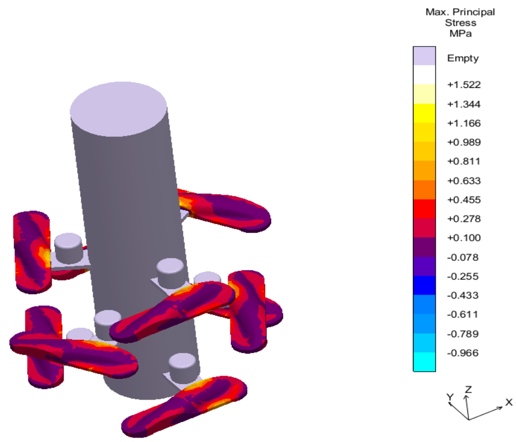

Fig. 44. Stress occurring during solidification for variant IV after 12 min

The last simulation also included tests of the stress changes in the casts occurring during the solidification process. The stresses are caused by the resistance of the mould to the solidifying casts and by differing temperature distributions at various points of the cooling material. The effect of these stresses can be the formation of cracks in the casts. The highest values are observed in the thin walls and in the areas where the running gates are attached.

After completing the solidification process simulation stage, pattern systems and moulds were prepared, then fired and filled with alloy AlSi11. The results of the mould and cast quality evaluation are presented below.

4. Discussion

4.1. Evaluation of ceramic mould quality

The ready quartz sand-based mould did not exhibit visible defects. The thickness of all the coatings after drying equaled about 1 cm. The aim of this quantity was protection from cracking while the patterns made on the injection moulded was being fired. The mould was well-dried.

The mould filled with loose quartz sand was fired in an electric furnace to a temperature of 720 °C. After its removal from the heated chamber, no cracks inside the pouring gate walls were observed. Next, the mould was filled with alloy AlSi11. The ceramic mould after casting is shown in Figure 45.

Fig. 45. Ceramic mould view after casting

On some casts, it was possible to observe mould cracks, formed at the long edge of the casts. The cause of the mould destruction during annealing was probably the increasing volume of polypropylene before its firing, under the effect of temperature. The mould slightly changed the colour of the coatings, which proved the occurrence of quartz sand transformations during the temperature increase in the furnace. The knocking-out of the casts from the mould ran easily, which also confirmed a good quality of its preparation.

4.2. Evaluation of cast quality

Figures 46 and 47 show exemplary Celtic stone casts


Fig. 46. Ceramic mould view after casting

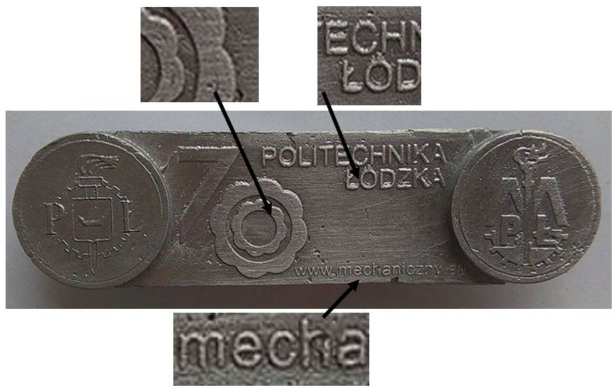

Fig. 47. Lower cast surface with inscriptions

On some casts, small flashes could be observed. This is likely related to uneven frothing of the pattern (the thin edges of the moulded piece had a uniform structure-no porosity). As a result of the pattern's firing, the material experiences a slight expansion in volume, which may lead to the formation of micro-cracks in the ceramic coatings. During casting, the weakened mould cracked in several places. It was noticeable that the cracks appeared at the long, thin edges. Flashes on the casts positioned at lower levels are larger than those on the upper part of the mould. This is caused by the uneven distribution of metallostatic pressure within the mould, which is greatest at the bottom. Additionally, small air bubbles were seen on the upper surface of the stone – Figure 46. The shape representation closely matches the pattern. The ceramic mould cavity accurately depicted the roundings and sharp edges of the cast. Inscriptions and logotypes, no more than a few tenths of a millimetre in height, on the flat surface, are clear and of good quality. Figure 47, marked with arrows, shows the decorative elements in the cast. Overall, measurements confirmed that there are virtually no deviations in the pattern dimensions.

5. Conclusions

Based on the studies conducted and the analysis of their results, the following conclusions regarding the assumptions and the outcomes obtained can be drawn.

- The selection of the gating system elements in the Replicast CS method is difficult due to the lack of specified requirements concerning the calculations. The determination of the appropriate pattern system is largely empirical in character. The estimation of the best variant is made based on the results of the simulations performed by means of the MAGMASOFT® v5.3 program.
- An important parameter during the determination of the gating system elements is the solidification module of the cast and the running gate. It can be inferred from the analysis of the performed simulations that the running gates must have a higher module value than the cast. If such an effect is impossible to obtain, feed bobs should be applied, in order to prolong the solidification time of the gates. In practice, this translates to eliminating the formation of defects in the casts.
- A single ceramic mould characterises a very good representation of the cast surface compared to the pattern. Also, polypropylene, as a material used for patterns, guarantees a very good representation of the edges and a dimension-shape stability, at the same time, not leaving solid parts after the firing.
- On some casts, it was possible to notice small flashes. This is probably connected with the non-uniform frothing of the pattern (on the thin edges, the moulded piece had a uniform structure – no porosity). As a result of the pattern's firing, the material undergoes a slight volume increase, which could be the cause of the formation of micro-cracks of the ceramic coatings. During the casting process, the weakened mould cracked in several places. It can be observed that the cracks were formed at the long thin edges.
- Despite the mould being cracked on the patterns' edges, the casting process was completed successfully. The representation of the shapes, surfaces and decoration elements was very good. The cause of the formed defects (small bubbles on the upper cast surface) was probably the minor discrepancies between the simulation parameters and those actually obtained, or the insufficient permeability of the ceramic mould.

The performed studies can be considered successful. The thematic scope is, however, so broad that further investigations should be performed concerning a change of the material type or the application of a higher amount of the blowing agent. Perhaps, with the modified conditions, the use of patterns produced on an injection moulded part will then turn out fully justified in the Replicast CS technology.

Acknowledgements

This publication was written at the Technical University of Liberec, Faculty of Mechanical Engineering with the support of the Institutional Endowment for the Long-Term Conceptual Development of Research Institutes, as provided by the Ministry of Education, Youth and Sports of the Czech Republic in the year 2025. The Authors would also like to thank the Lodz University of Technology, Department of Materials Engineering and Production Systems for the possibility of carrying out the research funded by their own resources.

References

[1] Pattnaik, S., Karunakar, D.B. & Jha, P.K. (2012). Developments in investment casting process—A review. *Journal of Materials Processing Technology*. 212(11), 2332-2348. https://doi.org/10.1016/j.jmatprotec.2012.06.003.

[2] Karwiński, A. & Żółkiewicz, Z. (2014). The research of properties of experimental ceramic layers. *Archives of Metallurgy and Materials*. 59(2), 703-705. DOI: 10.2478/amm-2014-0115.

[3] Ashton, M.C., Sharman, S.G. & Brookes, A.J. (1984). The replicast CS (Ceramic Shell) process. *Materials & Design*. 5(2), 66-75. https://doi.org/10.1016/0261-3069(84)90159-6.

[4] Karwiński, A., Haratym, R., Biernacki, R. & Soroczyński, A. (2014). Investment casting vs replicast cs considered in terms of the ceramic mould making and dimensional accuracy of castings. *Archives of Foundry Engineering*. 14(1), 45-48. DOI: 10.2478/afe-2014-0011.

[5] Technology card: Moplen HP500N

[6] Technical documentation: Plastronfoam B20

[7] Technical documentation: Injection moulder ARBURG ALLROUNDER 320 C 500-170 Golden Edition

[8] Technical documentation: printer 3D Zortrax M200

[9] Technical documentation: Z-HIPS, the material dedicated to the applied printer

[10] Technical documentation: The thermal plotter Megaplot P60

[11] Pisarek, B.P., Rapiejko, C., Szymczak, T. & Pacyniak, T. (2017). Effect of alloy additions on the structure and mechanical properties of the AlSi7Mg0. 3 alloy. *Archives of Foundry Engineering*. 17(1), 137-142. DOI: 10.1515/afe-2017-0025.

[12] Technical documentation: Factory of gear reducers and geared motors

[13] Technical documentation: The electric furnace APE 800

[14] Pacyniak, T., Gumienny, G., Szymczak, T. & Kurowska, B. (2017). Hypoeutectic Al-Si alloy doped with chromium, tungsten and molybdenum designated for pressure die casting. *Archives of Metallurgy and Materials*. 62(2), 1629-1635. DOI: 10.1515/amm-2017-0249.

[15] Rapiejko, C., Pisarek, B. & Pacyniak, T. (2014). Effect of Cr and V alloy additions on the microstructure and mechanical properties of AM60 magnesium alloy. *Archives of Metallurgy and Materials*. 59(2), 771-775. DOI: 10.2478/amm-2014-0128.

[16] Rapiejko, C., Pisarek, B., Czekaj, E. & Pacyniak, T. (2014). Analysis of AM60 and AZ91 alloy crystallisation in ceramic moulds by thermal derivative analysis (TDA). *Archives of Metallurgy and Materials*. 59(4), 1449-1455. DOI: 10.2478/amm-2014-0246.

[17] Rapiejko, C., Pisarek, B., Czekaj, E. & Pacyniak, T. (2014). Analysis of the crystallization of AZ91 alloy by thermal and derivative analysis method intensively cooled in ceramic shell. *Archives of Foundry Engineering.* 14(1), 97-102. DOI: 10.2478/afe-2014-0022.
[18] Szymczak, T., Pisarek, B., Rapiejko, C., Władysiak, R., Just, P., Kaczorowski, R., Gumienny, G., Januszewicz, B., Piątkowski, J. & Sinelnikov, V. (2025). The effect of Sr, Ti, and B on the crystallization process and mechanical properties of the AlSi9Cu3(Fe) alloy. *Materials*. 18(4), 882, 1-36. https://doi.org/10.3390/ma18040882.
[19] PN-EN 1706:2011. Aluminum and aluminum alloys. Castings. Chemical composition and mechanical properties.
[20] Allen, J. Romilly. (1904). *Celtic spirals from the book Celtic art in pagan and Christian times*. Retrieved October 1, 2025, from https://archive.org/details/celticartpagan00alleiala.
[21] Technological documentation of the foundry „ARMATURA", Lodz, Poland.